ELSEVIER

Chemical Engineering Journal 133 (2007) 343–354

Chemical Engineering Journal

www.elsevier.com/locate/cej

Stability and response of bioreactor: An analysis with reference to microbial reduction of SO_2

Susmita Dutta [a], Ranjana Chowdhury [b,*], Pinaki Bhattacharya [b]

[a] *Chemical Engineering Department, University of Calcutta, Kolkata 700009, India*
[b] *Chemical Engineering Department, Jadavpur University, Kolkata 700032, India*

Received 11 August 2006; received in revised form 19 January 2007; accepted 26 February 2007

Abstract

A continuous B. Braun fermenter undergoing the first stage of bioreduction of gaseous pollutant, SO_2—abiotically transformed to sulfite solution, using *Desulfotomaculum nigrificans*, purchased from NCIM, Pune (India), has been analysed both under steady and dynamic states. The kinetics of the microbial growth have been observed to face product inhibition in the entire range of inlet sulfite concentration of 0.904–1.696 g/dm^3. The kinetic parameters like maximum specific growth rate (μ_m), saturation constant (K_S) and product inhibition constant (K_P) have been evaluated by non-linear regression analysis and their values have been found to be 0.185 ks^{-1}, 6.512×10^{-3} g/dm^3 and 0.045 g/dm^3, respectively. The yield coefficient of generation of biomass with respect to the uptake of sulfite, $Y_{X/S}$, has been observed to vary non-linearly with the fractional conversion of sulfite and the functional relationship has been determined as $1.918 \exp(-1.984X_A)$. Under the present range of values of dilution rate (2.778×10^{-3} to 0.056 ks^{-1}), the steady state conversion of sulfite has been observed to lie in the range of 99.6–6.12%. Non-ideality, i.e., the extent of deviation from the ideal hydrodynamic behavior of the bioreactor has been assessed using a two-parameter model. The parameters of this model have been evaluated conducting step-type tracer experiments for residence time distribution (RTD) of inlet tracer molecules in the fermenter. The values of the non-ideal parameters indicate that the reactor behaves almost ideally under the present investigation. For a priori determination of the stable regime of operation of this biosystem, in general, global and local stability analyses have been done by the techniques of separatrices and linear analysis, respectively. The process dynamics and the control behavior of the system have been assessed by the analysis of its response with respect to step changes in the forcing functions, namely flow rate and the sulfite concentration in the inlet stream of the bioreactor.

Keywords: Bioreactor; Mathematical modelling; Dynamic simulation; Stability; Phase plane analysis; Response analysis

1. Introduction

Removal of gaseous pollutants by biological route is becoming increasingly important since the technique is most suitable in reducing the pollutant concentration in very low (ppm) level. A considerable amount of work has been carried out in identifying microorganisms suitable for such process [1,2]. Selection of a suitable bioreactor for such application demands proper stability and consistency study for their efficient operation. These analyses are also necessary from the aspect of process control of the reactors ensuring consistent and reliable performances. Literature survey shows that a limited number of papers have addressed such performance study, where majority of the authors have considered simplified reaction dynamics for stability analysis. Notably, a major contribution in this field has been made separately by several workers [3–15]. Application of those published pioneering techniques seems to be limited in bioprocess systems under investigation. Since in real time situation such pollutant removal processes follow rather complex routes, viz., shifting order reaction coupled with simultaneous substrate and product inhibition, etc., it is felt that a comprehensive stability analysis of bioreactor for such a system should be initiated in this line. On the other hand due to the generation of additional biomass with time, the viscosity of the reacting fluid increases and in many cases there may be a probability of formation of dead space in the system. Hence the dispersion of reacting species does not take place on a molecular scale as the reaction proceeds. Although the react-

* Corresponding author. Fax: +91 33 24146378.
E-mail address: ftbe_bon@yahoo.com (R. Chowdhury).

1385-8947/$ – see front matter © 2007 Elsevier B.V. All rights reserved.
doi:10.1016/j.cej.2007.02.029

ing mass may be regarded as perfectly mixed on a gross scale, on a molecular scale it may not be [16]. The deterioration in the quality of mixing may have a significant effect on reactor performance.

In the present investigation an attempt has been made to analyze the non-ideal behavior of a mixed flow bioreactor (chemostat) and the stability and consistency characteristics during transient condition using a biochemical system having product inhibition effect on the overall reaction rate. The system selected for such study is the first step of removal of SO_2 from flue gas through microbial route. In this step SO_2 has been converted to H_2S using sulfate-reducing bacteria, *Desulfotomaculum nigrificans*. As indicated by other investigator [17], this step is characterized by product inhibition, i.e., H_2S itself inhibits the bioprocess. However, published literature [15] shows that biochemical system involving product inhibition is susceptible to unusual dynamic behavior like oscillatory transition from one steady state to another, and sometimes sustained oscillation for an unfavourable period to reach a new steady state. Multiplicity, i.e., occurrence of multiple steady states corresponding to a single set of values of process parameters (similar to auto-thermal process) is also another unusual feature of such system. Therefore, an a priori knowledge of stable operating regime for such systems is a challenging demand for process engineers. In the present investigation a comprehensive analysis of the stability criteria of mixed flow bioreactor undergoing microbial conversion of SO_2 to H_2S has been presented. Local stability analysis has been performed by linear analysis while global stability of biosystem has been studied by phase plane analysis using the concept of separatrices. These analyses have helped in identifying different zones according to their stability characteristics in the parameter space with the dilution rate (D, ks^{-1}) and inlet substrate concentration ($C_{A,in}$, g/dm^3) as the main input variables.

While studying system dynamics it is an usual practice to study control action needed to maintain specified condition since sometimes unpredictable upsets in the operating conditions like fluctuation in pumping rate, change in flow patterns, inlet substrate concentration, etc., may occur. In the present investigation, after identification of appropriate parameter space, response analysis has been carried out by deliberately creating different step-type perturbations in the operating conditions. Inlet substrate concentration has been specifically selected as the forcing function in the present case. A series of programmed experiments on bioreduction of SO_2 to H_2S using *D. nigrificans*, has been performed. The experimental data, so evolved, have been compared with the simulated values. A reasonably good fit between experimental and simulated values indicates a potential application of the proposed model equations in the real time situation.

Moreover, non-ideal behavior of the bioreactor has also been investigated. A two-parameter model (reactor with bypass and dead volume) has been considered to analyze the real behavior of the bioreactor. Tracer technique is used to evaluate the parameters in the model.

2. Materials and methods

2.1. Microorganism (D. nigrificans)

Microorganism used in the present study was sulfate-reducing bacteria purchased from National Collection of Industrial Microorganism (NCIM), Pune, India.

2.2. Reactor

Fermentation using sulfite ions as substrate was carried out in a $2\,dm^3$ B. Braun fermenter (Biostat® B2) using *D. nigrificans*. The fermenter was an autoclavable glass vessel ($W \times H \times D$: 305 mm × 580 mm × 270 mm) with double jacket, stainless steel lid and baffle cage. The reactor was equipped with open temperature control system for the maintenance of constant operating temperature throughout the process. 180 W electronic motor was provided with the reactor for stirring the culture medium in the range of 50–1200 rpm.

2.3. Medium

Postgate medium was used for the growth of *D. nigrificans*. The medium was prepared following the protocol suggested by Postgate [17]. Composition of the medium is as follows: K_2HPO_4: 0.5 g; NH_4Cl: 1.0 g; Na_2SO_4: 1.0 g; $CaCl_2{\cdot}2H_2O$: 0.1 g; $MgSO_4{\cdot}7H_2O$: 2.0 g; Na-lactate (70%): 3.5 g; yeast extract: 1.0 g; distilled water: 980 ml; $FeSO_4{\cdot}7H_2O$: 0.5 g; distilled water: 10 ml; Na-thioglycollate: 0.1 g; ascorbic acid: 0.1 g; distilled water: 10 ml. All chemicals, unless otherwise stated, were of A.R. grade.

2.4. Acclimatization procedure

Working cultures of *D. nigrificans* were developed as follows. The culture was grown aseptically in Postgate medium in a $2\,dm^3$ B. Braun fermenter at pH 7.4 and 30 °C. The culture was purged with nitrogen to strip H_2S and maintain anaerobic conditions. After 86.4 ks, cells were harvested by centrifugation at 4900 rpm for 0.6 ks at 25 °C. The supernatant was discarded and cells were resuspended in sulfite medium where sulfate ions of Postgate medium had been substituted by sulfite ions. Sulfite ions act as the terminal electron acceptor. The resuspended cells were transferred back to the fermenter and grown anaerobically in this medium.

2.5. Experimental

2.5.1. Batch study

For the removal of SO_2, the bioscrubbing method was followed. To study the kinetics of the bioreduction of SO_2 by *D. nigrificans* in batch mode, sulfite ion, produced by the abiotic transformation of SO_2 gas, was used to substitute sulfate ions in Postgate medium. SO_2 gas was generated by the reaction of copper turnings with concentrated sulfuric acid at some elevated temperature. The generated gas was then dissolved in water to produce sulfurous acid. The concentration

of sulfurous acid so produced was determined iodometrically. The sulfurous acid solution was used to substitute sulfate ions (Na_2SO_4 and $MgSO_4{\cdot}7H_2O$) of Postgate medium. Several experimental runs were carried out in the 0.1 dm^3 volumetric flask varying the concentration of the limiting substrate, i.e., sulfite ions, in the range of 0.904–1.696 g/dm^3. The stirrer speed was kept constant at 100 rpm. The temperature and pH of the culture broth were maintained at $30 \pm 1\,^{\circ}C$ and 7.4, respectively. In all the cases, after a period of 259.2 ks, culture broth in fermenter turned black indicating the formation of sulfides (Fe^{2+}) as a result of reduction of sulfites by the action of *D. nigrificans*. Therefore, the experimental runs were carried out in each case for 259.2 ks. Samples were drawn periodically from the fermented broth and were analyzed for both H_2S and cell mass. Maximum conversion achieved in the batch study was about 99%. Yield coefficients ($Y_{X/S}$) were determined.

2.5.2. Flow system

Experiments in continuous mode were also conducted in a 2 dm^3 B. Braun fermenter (Biostat® B2). The bioreactor was fed with sterile medium using a peristaltic pump. The liquid product was also taken out of the fermenter at the same rate using another peristaltic pump. The reactor was initially filled with 1 dm^3 medium and inoculated with the culture. Dilution rate (D) was varied in the range of 2.778×10^{-3} to 0.056 ks^{-1} and the inlet concentration of limiting substrate, i.e., sulfite ions ($C_{A,in}$), was varied in the range of 0.904–1.696 g/dm^3. The stirrer speed was kept constant at 100 rpm. The temperature and pH of the culture broth were maintained at $30 \pm 1\,^{\circ}C$ and 7.4, respectively.

2.6. Tracer experiment

Potassium permanganate, the tracer, was injected in the system through step input. The tracer concentration in the effluent stream has been measured as a function of time using spectrophotometric method. Thus, residence time distribution (RTD) of the non-reacting substance, i.e., tracer was determined experimentally. Using the transient data of output tracer concentration, the values of model parameters namely α and β have been determined.

2.7. Analytical method

Biomass concentrations were measured by dry weight method. The culture broth was centrifuged at 4900 rpm for 0.6 ks. The cells were washed twice with distilled water. Aluminium cups containing the cell mass were left for 86.4 ks at 80 °C for drying. Finally the weight of cell mass was taken.

The concentrations of sulfurous acid were determined by iodometric method [18]. Determination of SO_2 concentration was made by West–Gaeke method [18] and the methylene blue procedure was used for the colorimetric determination of H_2S [2]. The concentration of tracer was measured using spectrophotometer (Spectrascan UV 2600, Chemito).

3. Theoretical analysis

3.1. Model equations

3.1.1. Determination of reaction kinetics

Before developing the model equations, kinetic nature of the bioconversion of SO_2 to H_2S is to be ascertained. In order to do that the growth curve (Fig. 1) of *D. nigrificans* in the initial sulfite concentration range of 0.904–1.696 g/dm^3 has been utilized to characterize the kinetic nature of the bioconversion reaction under investigation. It is evident from the figure that after the lag phase for each C_{A0}, initial concentration of substrate (g/dm^3) kept in reactor, instead of getting an exponential growth a linear growth region giving linear growth rate expression is obtained. This is clearly an indication that the overall growth rate of the present system is inhibited either by product or by substrate. To ascertain the type of inhibition, i.e., whether it is the substrate or product which inhibits, experiments have been conducted with different initial concentration of substrate (SO_2) and product (H_2S). It is evident from the dependence of specific growth rate on the initial substrate concentration and product that the system is inhibited by the product, i.e., H_2S. Similar observation and conclusion have also been made by Postgate [17]. Again in order to identify the nature of product inhibition, i.e., whether it is competitive or non-competitive type, product had been added initially in various concentrations to the cultures and the growth kinetics for each initial product concentration was studied. It was observed that the specific growth rate got decreased with the increase in the initial H_2S concentration indicating the presence of non-competitive product inhibition in the reacting system. Thus, the following classical kinetic equations have been attempted to explain the growth kinetics of the microorganism under study [19,20]:

$$\mu = \frac{\mu_m}{(1 + K_S/C_A)(1 + C_P/K_P)} \tag{1}$$

where

$$\frac{dC_B}{dt} = \mu C_B \tag{2}$$

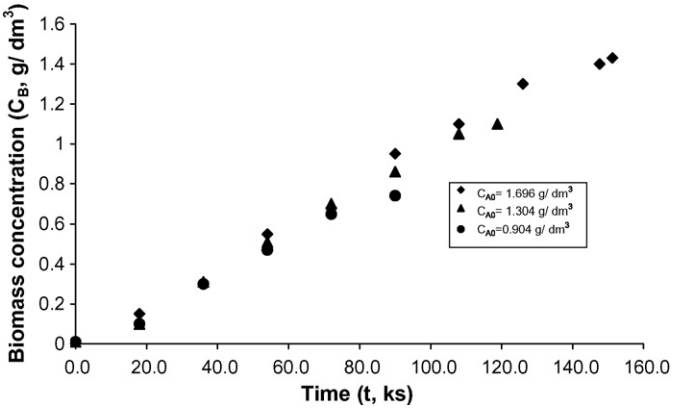

Fig. 1. Experimental concentration–time histories of biomass for bioreduction of sulfite during active growth phase for batch study in lab-scale fermenter with C_{A0} as a parameter. In all cases $C_{B0} = 0.01$ g/dm^3, temperature = 30 °C and pH 7.4.

Table 1
Values of different parameters

Parameters	Values
$C_{A0,max}$	2.000
$C_{B0,max}$	1.000
K_P	0.045
K_S	6.512×10^{-3}
$X_{A,max}$	0.996
α	0.95
β	0.05
η	1.918
μ_m	0.185
ρ	1.984

and

$$\frac{dC_A}{dt} = -\frac{dC_B/dt}{Y_{X/S}} \tag{3}$$

Initial conditions prevailing in the batch reactor are as follows:

at $t = 0$, $C_A = C_{A0}$, $C_B = C_{B0}$

where μ = specific growth rate, ks^{-1}; C_A = substrate concentration in the reactor at time t, g/dm^3; C_{A0} = initial concentration of substrate kept in the reactor, g/dm^3; C_B = biomass concentration in the reactor at time t, g/dm^3; C_{B0} = initial concentration of biomass kept in the reactor, g/dm^3; C_p = product concentration in the reactor at time t, g/dm^3; t = time, ks.

The kinetic parameters like maximum specific growth rate (μ_m, ks^{-1}), saturation constant (K_S, g/dm^3), and product inhibition constant (K_P, g/dm^3) have been evaluated by non-linear regression analysis method using the experimental data of batch operations (Table 1).

3.2. Computation of yield coefficient ($Y_{X/S}$)

In the present system yield coefficient ($Y_{X/S}$) is not expected to be constant since the growth rate is inhibited by its product. This leads to a judicious and thorough investigation on identifying the independent variable over which $Y_{X/S}$ depends so that the kinetic behavior can adequately be expressed. Since the system is product inhibited and also it is known that the yield coefficient is dependent on substrate consumption pattern, a unified approach in the present investigation has been made to describe yield coefficient as a function of fractional conversion of substrate (X_A) rather than concentration itself. An empirical equation showing the dependence of yield coefficient on the fractional conversion of substrate has now been assumed:

$$Y_{X/S} = \eta\, e^{-\rho X_A} \tag{4}$$

In order to calculate the dimensionless empirical constants η and ρ, a non-linear regression analysis has been carried out using the experimental data mentioned above.

3.3. Model equations for bioreactor

Under real situation, the chemostat may not behave ideally due to the generation of dead space, bypassing of a fraction of reacting stream without conversion, etc. To account for the probable non-ideality in the chemostat, analysis of reactor behavior has been done both from ideal and non-ideal perspectives.

3.3.1. Ideal

Simulation of continuous type fermenter has been carried out using the following data and assumptions:

1. As the biochemical process takes place in an ideal mixed flow bioreactor, no spatial variation of parameters exists.
2. The reaction is a unimolecular one as evident from the kinetic study carried out by Postgate [17].
3. Physicochemical properties, viz., density, viscosity, etc., of the reaction broth do not change appreciably with the propagation of reaction.

The dimensionless material balance equations for substrate and biomass for a mixed flow bioreactor (chemostat) under steady state condition are as follows:

$$-\frac{D^* C^*_{A,in} X^*_m}{C^*_{A0}} + D^* X^*_m - D^* X^*_{AS} + \frac{K^*_P C^*_{BS} X^{*2}_m (X^*_m - X^*_{AS})}{\eta^* e^{-\rho^* X^*_{AS}} \Phi^*_S} = 0 \tag{5}$$

$$-D^* C^*_{BS} + \frac{K^*_P C^*_{BS} X^*_m C^*_{A0} (X^*_m - X^*_{AS})}{\Phi^*_S} = 0 \tag{6}$$

where

$$C^*_{A0} = \frac{C_{A0}}{C_{A0,max}}, \quad C^*_{A,in} = \frac{C_{A,in}}{C_{A0,max}}, \quad C^*_{BS} = \frac{C_{BS}}{C_{B0,max}}, \quad D^* = \frac{D}{\mu_m}, \quad K^*_P = \frac{K_P}{C_{A0,max}}, \quad X^*_{AS} = \frac{X_{AS}}{X_{A,max}}, \quad X^*_m = \frac{1}{X_{A,max}}, \quad \eta^* = \frac{\eta C_{A0,max}}{C_{B0,max}}, \quad \rho^* = \rho X_{A,max}$$

and $C_{A0,max}$ = maximum initial concentration of substrate kept in the reactor, g/dm^3; C_{BS} = steady state value of biomass concentration in outlet stream, g/dm^3; $C_{B0,max}$ = maximum initial concentration of biomass kept in the reactor, g/dm^3; X_{AS} = fractional conversion of substrate corresponding to steady state value; $X_{A,max}$ = maximum fractional conversion of substrate.

The expression of Φ^*_S is, thus, obtained:

$$\Phi^*_S = (\alpha_1 + \beta_1 C^*_{A0} - \delta C^*_{A0} X^*_{AS} + \gamma C^*_{A0} X^*_{AS} + X^*_m C^{*2}_{A0} X^*_{AS} - C^{*2}_{A0} X^{*2}_{AS})$$

where

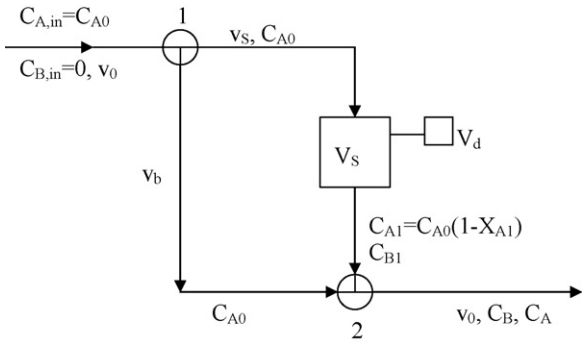

Fig. 2. Schematic diagram of real chemostat modeled with dead space and bypass [16].

$$\alpha_1 = \frac{K_S K_P}{C_{A0,max}^2 X_{A,max}^2}, \qquad \beta_1 = \frac{K_P}{C_{A0,max} X_{A,max}^2},$$

$$\delta = \frac{K_P}{C_{A0,max} X_{A,max}}, \qquad \gamma = \frac{K_S}{C_{A0,max} X_{A,max}}$$

3.3.2. Non-ideal

A real chemostat having total volume V (dm^3) has been modeled as a combination of an ideal chemostat of volume V_s (dm^3), a dead zone of volume V_d (dm^3), and a bypass with a volumetric flow rate v_b (dm^3/ks) (Fig. 2). Tracer experiment has been conducted under non-reacting condition. By determining the residence time distribution (RTD) of tracer the model parameters namely, α and β have been evaluated.

In Fig. 2 the bypass stream and effluent stream from the reaction volume are mixed at point 2. To determine the reactor hydrodynamics, a balance on substrate and biomass around this point and on simplification one should get

$$C_A = \beta C_{A0} + C_{A0}(1-\beta)(1-X_{A1}) \tag{7}$$

$$C_B = (1-\beta) C_{B1} \tag{8}$$

where, $\beta = v_b/v_0$ = fraction of unconverted inlet feed stream; C_{B1} = biomass concentration at steady state as shown in Fig. 2, g/dm^3; X_{A1} = fractional conversion of substrate at steady state as shown in Fig. 2; v_0 = volumetric flow rate of inlet stream to the reactor (dm^3/ks).

For the bioreduction of SO_2, mass balance of sulfite and biomass on V_s, the completely stirred volume of the reactor, under steady state condition gives

$$\frac{(1-\beta)DX_{A1}}{\alpha} - \frac{\mu_m K_P C_{B1}(1-X_{A1})}{\eta\, e^{-\rho X_{A1}}(K_S K_P + K_P C_{A0} + C_{A0} K_S X_{A1} - C_{A0} K_P X_{A1} + C_{A0}^2 X_{A1} - C_{A0}^2 X_{A1}^2)} = 0 \tag{9}$$

$$-\frac{(1-\beta)DC_{B1}}{\alpha} + \frac{\mu_m K_P C_{A0}(1-X_{A1}) C_{B1}}{(K_S K_P + K_P C_{A0} + C_{A0} K_S X_{A1} - C_{A0} K_P X_{A1} + C_{A0}^2 X_{A1} - C_{A0}^2 X_{A1}^2)} = 0 \tag{10}$$

where $\alpha = V_s/V$ = fraction of useful volume.

3.4. Determination of model parameters α and β

In the present article the non-ideality of the reactor has been assessed using two-parameter model considering the hydrodynamics of the chemostat as a combination of perfectly stirred reactor, dead space and bypass. A non-reacting tracer has been injected as a positive-step input. The tracer concentration in the effluent stream has been measured as a function of time. The characteristic equation for determining the values of α and β is as follows:

$$\ln\frac{C_{T0}}{C_{T0}-C_T} = \ln\frac{1}{1-\beta} + \left(\frac{1-\beta}{\alpha}\right)\frac{t}{\tau} \tag{11}$$

where C_{T0} = concentration of tracer in the inlet stream, g/dm^3; C_T = concentration of tracer in the exit stream, g/dm^3; $\tau = V/v_0$.

Thus, $\ln C_{T0}/(C_{T0}-C_T)$ has been plotted against time t (figure not shown) and from the slope and intercept of the straight line, the values of two parameters α and β have been determined. Values of α and β have been given in Table 1.

3.4.1. Stability analysis

It is evident from the values of model parameters (α and β) of non-ideality that the present reactor behaves ideally. Thus, the system equations, valid for ideal situation have been used for the subsequent analysis of the reactor.

The non-dimensionalized unsteady state equations for ideal chemostat are as follows,

$$\frac{dX_A^*}{d\theta} = -\frac{D^* C_{A,in}^* X_m^*}{C_{A0}^*} + D^* X_m^* - D^* X_A^* + \frac{K_P^* C_B^* X_m^{*2}(X_m^* - X_A^*)}{\eta^*\, e^{-\rho^* X_A^*} \Phi^*} \tag{12}$$

$$\frac{dC_B^*}{d\theta} = -D^* C_B^* + \frac{K_P^* C_B^* X_m^* C_{A0}^*(X_m^* - X_A^*)}{\Phi^*} \tag{13}$$

where $C_B^* = C_B/C_{B0,max}$, $X_A^* = X_A/X_{A,max}$, $\theta = t\mu_m$ and $\Phi^* = (\alpha_1 + \beta_1 C_{A0}^* - \delta C_{A0}^* X_A^* + \gamma C_{A0}^* X_A^* + X_m^* C_{A0}^{*2} X_A^* - C_{A0}^{*2} X_A^{*2})$.

The non-linear nature of the above non-dimensionalized characteristic equations (Eqs. (12) and (13)) may lead to the multiplicity in a mixed flow bioreactor. This means that for a given set of feed conditions and operating parameters the reactor may exhibit one or more ambiguous steady states. The existence of multiplicity in a biochemical system is usually verified by studying operating diagrams [15].

It is evident that for systematic study of any reactor behavior, the steady state values for each operating condition are to be established first and then stability analysis will have to be made to find its nature. A steady state is stable if, for initial conditions near the steady state all transient responses converge to it [10]. On the other hand if they diverge, the steady state under investigation becomes unstable. The linear stability anal-

ysis is important in this respect as it gives the clear picture of the stability of each steady state and information about the local dynamics. However, one must keep in mind that such analysis is suitable only near the steady states. For global behavior, generation of phase plane and their subsequent analysis is absolutely necessary.

3.5. Local stability analysis

Local stability of the system has been assessed following the technique of linear stability analysis. As a general rule for linear stability analysis, all non-linear model equations must be linearized first. In the present investigation the model equations so evolved, are highly non-linear in nature and need linearization. According to linear stability analysis, a steady state is considered to be stable if all the transients converge to it, when initial conditions are localized/restricted in the vicinity of the steady state.

For a particular feed condition the steady state values of X^*_{AS} and C^*_{BS} have been found by solving Eqs. (5) and (6) using non-linear root finding technique.

In the present case, which represents a general multivariable non-linear autonomous system, the required Jacobian matrix is formed truncating the higher order terms to get linear form of Taylor series.

Thus, the Jacobian matrix, $\tilde{J}$, of Eqs. (12) and (13) is as follows:

$$\tilde{J} = \left| \begin{array}{cc} \dfrac{\partial \dot{C}^*_B}{\partial C^*_B} & \dfrac{\partial \dot{C}^*_B}{\partial X^*_A} \\ \dfrac{\partial \dot{X}^*_A}{\partial C^*_B} & \dfrac{\partial \dot{X}^*_A}{\partial X^*_A} \end{array} \right|_{SS} \tag{14}$$

The eigen values (λ) can be determined by solving the following characteristic equation:

$$|\tilde{J} - \lambda \tilde{I}| = 0 \tag{15}$$

where $\tilde{I}$ = unit vector.

If after computation of eigen values λs' (in the present case two in number) from the above equation it is observed that if any of the eigen values is positive, then steady state is unstable whereas the negative real values of λ indicate the stable behavior of steady state under study. On the other hand if the eigen value is a complex number, oscillation is expected around the steady state. The oscillation is of damped or diverging pattern depending on negative and positive nature of the real part of the eigen values, respectively.

3.6. Global stability analysis

Although local behavior of steady states is to be studied using linear analysis technique, global/general stability analysis of the biosystem may be done using phase plane analysis. Phase plane analysis has been done by dividing non-dimensionalized cell mass balance equation (Eq. (13)) by that of substrate mass balance equation (Eq. (12)), to eliminate the incremental time $d\theta$ [10,11]. The resulting differential equation becomes as follows:

$$\frac{dC^*_B}{dX^*_A} = \frac{[(K^*_P C^*_{A0} X^*_m (X^*_m - X^*_A)/\Phi^*) - D^*]C^*_B}{[D^*(X^*_m - (C^*_{A,in} X^*_m / C^*_{A0}) - X^*_A) + K^*_P C^*_B X^{*2}_m (X^*_m - X^*_A)/\eta^* \, e^{-\rho^* X^*_A} \Phi^*]} \tag{16}$$

In the phase space, the oriented curve described by the movement of any point in it is known as phase trajectory. The trajectory consisting of a single point corresponds to a rest point or a stationary point in the space [21]. In the system under consideration, a unique rest point, i.e., steady state is obtained for the preset values of D^* and $C^*_{A,in}$. This is obtained by solving the following equations:

$$\text{Line A}: \quad \frac{K^*_P C^*_{A0} X^*_m (X^*_m - X^*_A)}{\Phi^*} = D^* \tag{17}$$

$$\text{Line B}: \quad X^*_A = \left(X^*_m - \frac{C^*_{A,in} X^*_m}{C^*_{A0}} \right) + \frac{C^*_B X^*_m}{C^*_{A0} \eta^* \, e^{-\rho^* X^*_A}} \tag{18}$$

$$\text{Line C}: \quad D^* \left(X^*_m - \frac{C^*_{A,in} X^*_m}{C^*_{A0}} - X^*_A \right) = \frac{K^*_P C^*_B X^{*2}_m (X^*_m - X^*_A)}{\eta^* \, e^{-\rho^* X^*_A} \Phi^*} \tag{19}$$

The values of C^*_A corresponding to those of X^*_A have been used to generate the phase plane. While converting X^*_A to C^*_A, the following relation has been used.

$$C^*_A = \frac{C^*_{A0}}{X^*_m}(X^*_m - X^*_A) \tag{20}$$

For autonomous systems of the present type it is usually possible to identify surfaces, called separatrices, in the phase space in which the behavior patterns of all phase trajectories in one separatrix are distinct and identical. In the present work the phase space (C^*_B, C^*_A) has been divided into six separatrices using the equations of lines A–C (Eqs. (17)–(19)). The division has been done by examining the behavior of trajectories, which start at different initial conditions (C^*_{B0}, C^*_{A0}) (where $C^*_{B0} = C_{B0}/C_{B0,max}$, $C^*_{A0} = C_{A0}/C_{A0,max}$) and ultimately converge to the steady state/rest point.

3.6.1. Response of the system against step change

The response pattern of concentrations of biomass and substrate in the time domain may be generated by the following analysis [22]:

On introduction of the perturbation variables (X^{*p}_A, C^{*p}_B, $C^{*p}_{A,in}$ and D^{*p}) in the Taylor series expansion of dimensionless variables X^*_A, C^*_B, $C^*_{A,in}$ and D^* in Eqs. (12) and (13) around their steady state and after truncation of higher order partial derivatives w.r.t. time, one gets,

$$\frac{dX^{*p}_A}{d\theta} = a_{11} X^{*p}_A + a_{12} C^{*p}_B + a_{13} C^{*p}_{A,in} + a_{14} D^{*p} \tag{21}$$

$$\frac{dC^{*p}_B}{d\theta} = a_{21} X^{*p}_A + a_{22} C^{*p}_B + a_{23} C^{*p}_{A,in} + a_{24} D^{*p} \tag{22}$$

where $X_A^{*p} = (X_A^* - X_{AS}^*)$, $C_B^{*p} = (C_B^* - C_{BS}^*)$, $C_{A,in}^{*p} = (C_{A,in}^* - C_{A,inS}^*)$, $D^{*p} = (D^* - D_S^*)$, $C_{A,inS}^* = C_{A,inS}/C_{A0,max}$, $D_S^* = D_S/\mu_m$ and $C_{A,inS}$ = substrate concentration in feed corresponding to steady state, g/dm^3; D_S = dilution rate corresponding to steady state, ks^{-1}.

The expressions of coefficients (a_{11}–a_{24}) are as follows:

$$a_{11} = -D_S^* + \frac{K_P^* C_{BS}^* X_m^{*2}\{\phi + \rho^*(X_m^* - X_{AS}^*)\Phi_S^*\}}{\eta^* \, e^{-\rho^* X_{AS}^*} \Phi_S^{*2}} \quad (22a)$$

$$a_{12} = \frac{K_P^* X_m^{*2}(X_m^* - X_{AS}^*)}{\eta^* \, e^{-\rho^* X_{AS}^*} \Phi_S^*} \quad (22b)$$

$$a_{13} = -\frac{D_S^* X_m^*}{C_{A0}^*} \quad (22c)$$

$$a_{14} = \left(X_m^* - \frac{C_{A,inS}^* X_m^*}{C_{A0}^*} - X_{AS}^* \right) \quad (22d)$$

$$a_{21} = \frac{K_P^* C_{A0}^* C_{BS}^* X_m^* \phi}{\Phi_S^{*2}} \quad (22e)$$

$$a_{22} = -D_S^* + \frac{K_P^* X_m^* C_{A0}^* (X_m^* - X_{AS}^*)}{\Phi_S^*} \quad (22f)$$

$$a_{23} = 0 \quad (22g)$$

$$a_{24} = -C_{BS}^* \quad (22h)$$

where $\phi = (-\alpha - \gamma C_{A0}^* X_m^* - X_m^{*2} C_{A0}^{*2} - C_{A0}^{*2} X_{AS}^{*2} + 2C_{A0}^{*2} X_{AS}^* X_m^*)$.

Now the open loop transfer functions of this multivariable system have been determined considering $C_{A,in}^*$ and D^* as forcing functions. Mathematically these can be expressed as follows:

$$X_{A(S)}^{*p} = G_{11} C_{A,in(S)}^{*p} + G_{12} D_{(S)}^{*p} \quad (23)$$

$$C_{B(S)}^{*p} = G_{21} C_{A,in(S)}^{*p} + G_{22} D_{(S)}^{*p} \quad (24)$$

where $X_{A(S)}^{*p}$, $C_{B(S)}^{*p}$ are Laplace transform of X_A^{*p}, C_B^{*p} and G_{11}, G_{12}, G_{21} and G_{22} are all transfer functions. Expressions of them are as follows:

$$G_{11} = \left[\frac{a_{13}(S - a_{22}) + a_{12}a_{23}}{\psi} \right] \quad (25)$$

$$G_{12} = \left[\frac{a_{14}(S - a_{22}) + a_{12}a_{24}}{\psi} \right] \quad (26)$$

$$G_{21} = \left[\frac{a_{23}(S - a_{11}) + a_{13}a_{21}}{\psi} \right] \quad (27)$$

$$G_{22} = \left[\frac{a_{24}(S - a_{11}) + a_{14}a_{21}}{\psi} \right] \quad (28)$$

where

$$\psi = S^2 - (a_{11} + a_{22})S + a_{11}a_{22} - a_{12}a_{21} \quad (29)$$

Applying fractional step inputs (σ), the concentration profiles of substrate and biomass in the time domain are obtained by inverse Laplace transformation. The equations representing the time history of concentrations of substrate and biomass in response to fractional step inputs are as follows:

$$X_A^{*p}(\theta) = A_1 + B_1 \, e^{\xi\theta} \cos(\nu\theta) + \left(\frac{B_1\xi + C_1}{\nu} \right) e^{\xi\theta} \sin(\nu\theta) \quad (30)$$

$$C_B^{*p}(\theta) = A_2 + B_2 \, e^{\xi\theta} \cos(\nu\theta) + \left(\frac{B_2\xi + C_2}{\nu} \right) e^{\xi\theta} \sin(\nu\theta) \quad (31)$$

where $\xi = (a_{11} + a_{22})/2$ and $\nu = \sqrt{a_{11}a_{22} - a_{12}a_{21} - \xi^2}$.

A_1, A_2, B_1, B_2, C_1 and C_2 are constants whose expressions are given in Table 2.

4. Results and discussions

The biomass concentrations obtained experimentally in batch mode of operation varying C_{A0} in the range of 0.904–1.696 g/dm^3 have been plotted against reaction propagation time (Fig. 1) during active growth phase only. Fig. 3 depicts the concentration–time histories of substrate obtained experimentally during active growth phase in batch study of bioreduction of sulfite using *D. nigrificans* by varying initial substrate concentration (C_{A0}) in the range of 0.904–1.696 g/dm^3. From the close observation of the Fig. 1 it is evident that after the lag phase for each C_{A0} instead of getting an exponential growth a linear growth region giving linear growth rate expression is obtained. Evidently this is a clear indication of effect of product inhibition on the growth kinetics. However, substrate concentration follows an exponential time history. In the present case H_2S, one of the major products, becomes toxic to biomass as it precipitates out Fe^{2+}, an essential micronutrient for growth of biomass [17]. Furthermore, as discussed earlier (under Section 3) the product inhibition in the present case is non-competitive in nature. As a result an attempt has been made to fit the experimental data in non-competitive product inhibited model. The kinetic parameters like maximum specific growth rate (μ_m), saturation constant (K_S), and product inhibition constant (K_P) have been evaluated using the experimental data by non-linear regression

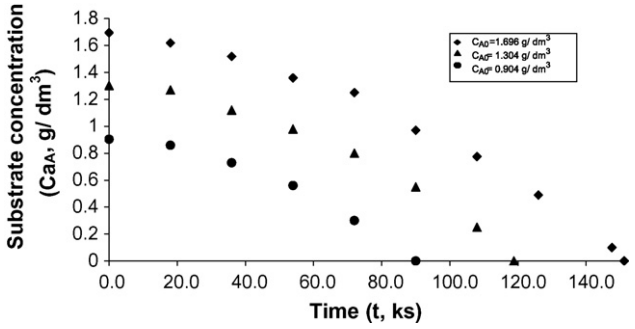

Fig. 3. Experimental concentration–time histories of substrate for bioreduction of sulfite during active growth phase for batch study in lab-scale fermenter with C_{A0} as a parameter. In all cases C_{B0} = 0.01 g/dm^3, temperature = 30 °C and pH 7.4.

Table 2
The expressions of A_1, A_2, B_1, B_2, C_1 and C_2 taking $C^*_{A,in}$ and D^* as forcing functions

Forcing function	A_1	A_2	B_1	B_2	C_1	C_2
$C^*_{A,in}$	$\sigma(a_{12}a_{23} - a_{13}a_{22})/(a_{11}a_{22} - a_{12}a_{21})$	$\sigma(a_{13}a_{21} - a_{11}a_{23})/(a_{11}a_{22} - a_{12}a_{21})$	$-A_1$	$-A_2$	$\sigma(a_{11}a_{12}a_{23} - a_{12}a_{13}a_{21} + a_{12}a_{22}a_{23} - a_{13}a_{22}^2)/(a_{11}a_{22} - a_{12}a_{21})$	$\sigma(a_{11}a_{13}a_{21} - a_{12}a_{21}a_{23} + a_{13}a_{21}a_{22} - a_{23}a_{11}^2)/(a_{11}a_{22} - a_{12}a_{21})$
D^*	$\sigma(a_{12}a_{24} - a_{14}a_{22})/(a_{11}a_{22} - a_{12}a_{21})$	$\sigma(a_{14}a_{21} - a_{11}a_{24})/(a_{11}a_{22} - a_{12}a_{21})$	$-A_1$	$-A_2$	$\sigma(a_{11}a_{12}a_{24} - a_{12}a_{14}a_{21} + a_{12}a_{22}a_{24} - a_{14}a_{22}^2)/(a_{11}a_{22} - a_{12}a_{21})$	$\sigma(a_{11}a_{14}a_{21} - a_{12}a_{21}a_{24} + a_{14}a_{21}a_{22} - a_{24}a_{11}^2)/(a_{11}a_{22} - a_{12}a_{21})$

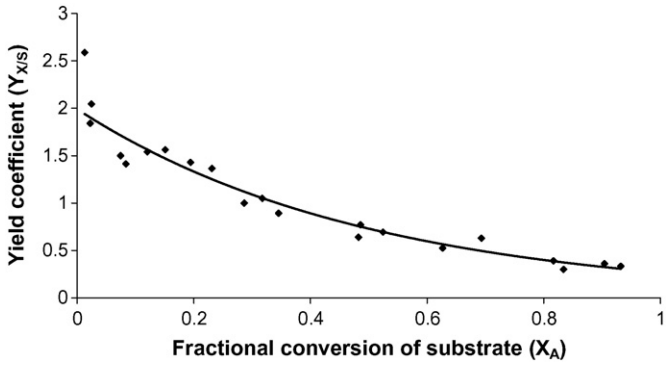

Fig. 4. Variation of yield coefficient with fractional conversion of substrate in the initial substrate concentration range of 0.904–1.696 g/dm^3.

analysis method. The values of μ_m, K_S, K_P are given in Table 1. In the plot of yield coefficient versus fractional conversion of substrate (Fig. 4) the yield coefficient ($Y_{X/S}$) has been observed to decrease exponentially with the fractional conversion of substrate for different values of initial substrate concentration in the range of 0.904–1.696 g/dm^3. This evidently indicates that $Y_{X/S}$ is solely dependent on X_A and the functionality is unaffected by the values of initial substrate concentration. Therefore, the exponential relationship between $Y_{X/S}$ and the fractional conversion of substrate (X_A) has been sought and has been determined by non-linear regression analysis method. The values of constants η and ρ of the regression equation (4) have been shown in Table 1 (index of correlation: 0.9589). The differential mass balance equations of biomass and substrate (sulfite), i.e., Eqs. (2) and (3) have been solved numerically using fourth-order Runge Kutta method with the aid of those kinetic parameters and the results are shown in Figs. 5 and 6. The experimental results are also superimposed on the corresponding curves. From the close observation of Figs. 5 and 6, it is evident that the experimental data are in good agreement with the simulated predictions of reaction engineering behavior incorporating product inhibition kinetics (the index of correlation for the concentration–time histories of biomass: 0.9938–0.9995; the index of correlation for the concentration–time histories of substrate: 0.9977–9993). Thus, this may be inferred that the system follows product inhibited growth under the present range of values of parameters studied.

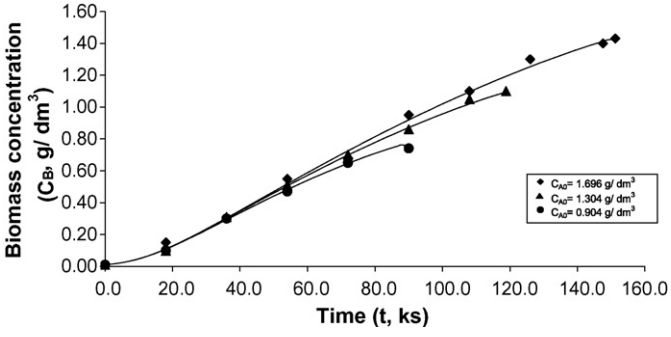

Fig. 5. Simulated (lines) and experimental (points) concentration–time histories of biomass for bioreduction of sulfite during active growth phase for batch study in lab-scale fermenter with C_{A0} as a parameter. In all cases $C_{B0} = 0.01$ g/dm^3, temperature = 30 °C and pH 7.4.

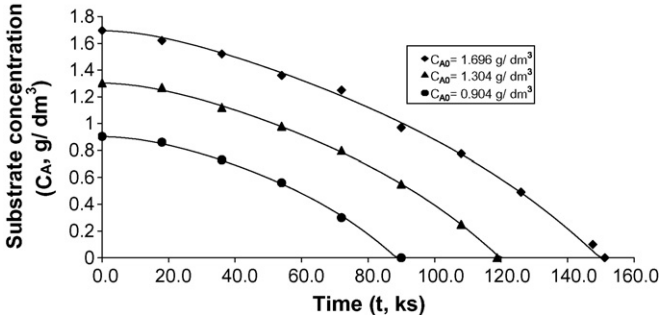

Fig. 6. Simulated (lines) and experimental (points) concentration–time histories of substrate for bioreduction of sulfite during active growth phase for batch study in lab-scale fermenter with C_{A0} as a parameter. In all cases $C_{B0} = 0.01$ g/dm^3, temperature = 30 °C and pH 7.4.

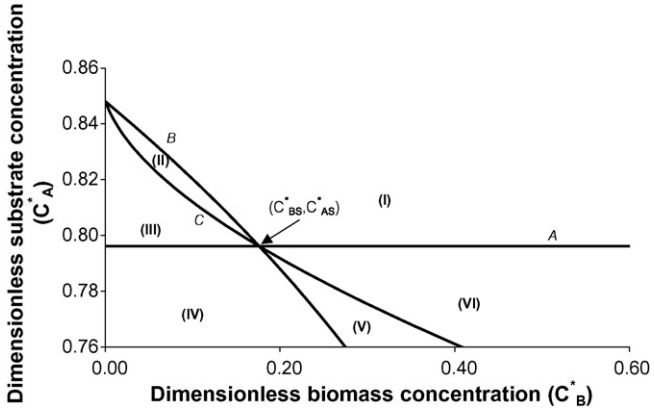

Fig. 7. The phase plane behavior of a mixed flow bioreactor with product inhibited kinetics. Lines A–C delineate the six separatrices (I–VI) for $D^* = 0.299$, $C^*_{A,in} = 0.848$.

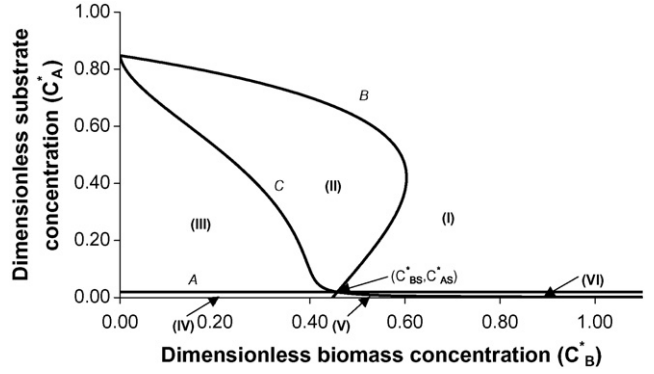

Fig. 8. The phase plane behavior of a mixed flow bioreactor with product inhibited kinetics. Lines A–C delineate the six separatrices (I–VI) for $D^* = 0.023$, $C^*_{A,in} = 0.848$.

4.1. Local analysis

Different steady state values of dimensionless substrate concentration, $C^*_{AS}[= C^*_{A0}/X^*_m(X^*_m - X^*_{AS})]$ and biomass concentration, $C^*_{BS}[= C_{BS}/C_{B0,max}]$ corresponding to present values of non-dimensional dilution rate and inlet substrate concentration have been obtained solving Eqs. (5) and (6). Local stability of each steady state has been analyzed by linear analysis technique. The eigen values of characteristic equation (Eq. (15)) corresponding to the steady states have been obtained by varying the values of D^* and $C^*_{A,in}$ and tabulated in Table 3. The analysis has been done for the values of D^* in the range of 0.015 and 0.299 and those of $C^*_{A,in}$ in the range of 0.452 and 0.848. From Table 3, it is evident that within the range of the variables studied, eigen values have negative real magnitudes indicating the occurrence of stable steady states.

4.2. Global stability analysis

In Figs. 7 and 8 the division of (C^*_B, C^*_A) plane into six separatrices using the lines A–C for two different D^* values (0.299 and 0.023, respectively) have been shown. For both the cases the value of $C^*_{A,in}$ is 0.848. For $D^* = 0.299$ and $C^*_{A,in} = 0.848$ the rest point has co-ordinates $C^*_{BS} = 0.176$ and $C^*_{AS} = 0.796$. The behavior of phase trajectories starting from randomly chosen initial conditions $P(C^*_{B0}, C^*_{A0})$ in each of the six separatrices on the phase plane are shown in Fig. 9. Convergence of trajectories starting from each separatrix to the rest point reconfirms the stability of the steady state. The approaching nature of phase trajectories with respect to biomass and substrate in six separatrices are given in Table 4. By similar analysis with $D^* = 0.023$, the coordinates of the rest point have been found to be (0.457, 0.019). Phase trajectories with the starting points $P(C^*_{B0}, C^*_{A0})$ situated in each separatrix have been observed to converge to

Table 3
Eigen values for different operating conditions

D^*	$C^*_{A,in}$	C^*_{BS}	C^*_{AS}	λ_1	λ_2
0.015	0.452	2.393×10^{-1}	1.511×10^{-3}	−1.528	−4.586
0.015	0.652	3.454×10^{-1}	2.667×10^{-3}	−1.005	−3.014
0.015	0.848	4.497×10^{-1}	4.504×10^{-3}	-5.899×10^{-1}	−1.769
0.023	0.452	2.399×10^{-1}	2.935×10^{-3}	-9.061×10^{-1}	−2.718
0.023	0.652	3.474×10^{-1}	6.653×10^{-3}	-3.590×10^{-1}	−1.077
0.023	0.848	4.574×10^{-1}	1.931×10^{-2}	-7.011×10^{-2}	-2.103×10^{-1}
0.045	0.452	2.531×10^{-1}	2.835×10^{-2}	-3.673×10^{-2}	-1.101×10^{-1}
0.045	0.652	4.328×10^{-1}	1.857×10^{-1}	-1.371×10^{-2}	-3.843×10^{-2}
0.045	0.848	6.003×10^{-1}	3.774×10^{-1}	-2.133×10^{-2}	-5.654×10^{-2}
0.299	0.452	1.578×10^{-1}	4.004×10^{-1}	-2.211×10^{-1}	-6.629×10^{-1}
0.299	0.652	1.697×10^{-1}	6.002×10^{-1}	-2.317×10^{-1}	-6.939×10^{-1}
0.299	0.848	1.762×10^{-1}	7.961×10^{-1}	-2.373×10^{-1}	-7.101×10^{-1}

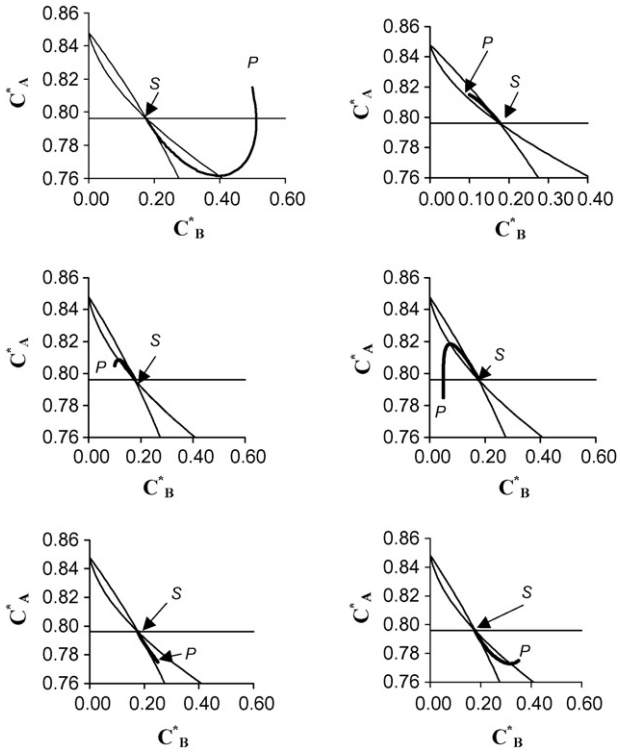

Fig. 9. The transient response of (C^*_B, C^*_A) in each of the six separatrices in the (C^*_B, C^*_A) phase plane for $D^* = 0.299$, $C^*_{A,in} = 0.848$. The coordinates of P are (C^*_{B0}, C^*_{A0}) and coordinates of S are (C^*_{BS}, C^*_{AS}).

Table 4
Classification of the transient response of (C^*_B, C^*_A) in each of the six separatrices in the (C^*_B, C^*_A) phase plane for $D^* = 0.299$, $C^*_{A,in} = 0.848$

(C^*_{B0}, C^*_{A0}) in separatrice	Behavior of ($C^*_B(\theta)$)	Behavior of ($C^*_A(\theta)$)
I	Overshoot	Underswing
II	Monotonic increase	Monotonic decrease
III	Monotonic increase	Overshoot
IV	Underswing	Overshoot
V	Monotonic decrease	Monotonic increase
VI	Monotonic decrease	Underswing

the rest point (Fig. 10) and thus the stability of the steady state is confirmed. The characteristics of phase trajectories regarding substrate and biomass in six separatrices are given in Table 5.

Table 5
Classification of the transient response of (C^*_B, C^*_A) in each of the six separatrices in the (C^*_B, C^*_A) phase plane for $D^* = 0.023$, $C^*_{A,in} = 0.848$

(C^*_{B0}, C^*_{A0}) in separatrice	Behavior of ($C^*_B(\theta)$)	Behavior of ($C^*_A(\theta)$)
I	Overshoot	Underswing
II	Overshoot	Underswing
III	Overshoot	Combination of overshoot and underswing
IV	Overshoot	Combination of overshoot and underswing
V	Monotonic decrease	Monotonic increase
VI	Monotonic decrease	Underswing

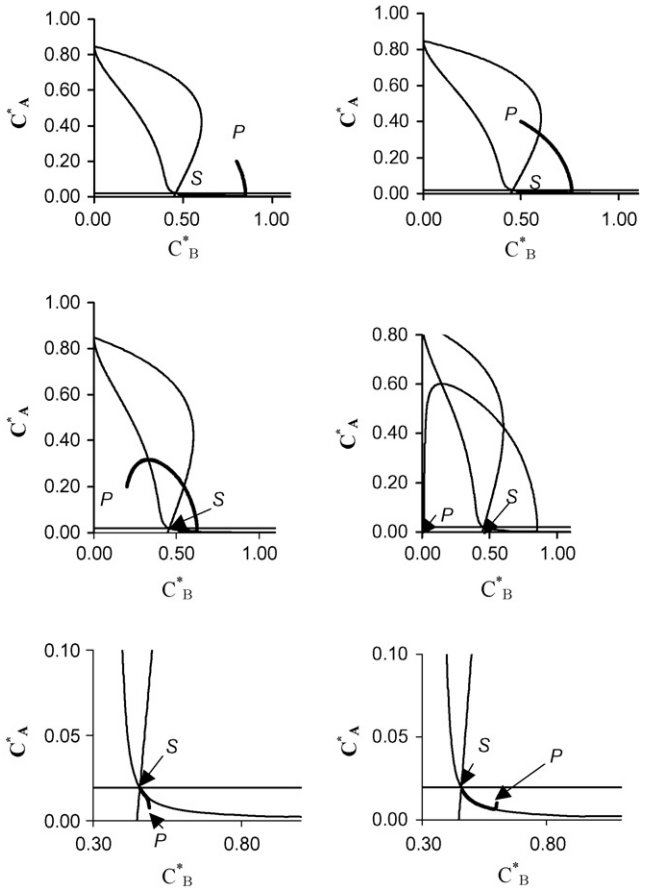

Fig. 10. The transient response of (C^*_B, C^*_A) in each of the six separatrices in the (C^*_B, C^*_A) phase plane for $D^* = 0.023$, $C^*_{A,in} = 0.848$. The coordinates of P are (C^*_{B0}, C^*_{A0}) and coordinates of S are (C^*_{BS}, C^*_{AS}).

4.3. Response analysis

To assess the system response to perturbation, transient response of the biosystem operating under different stable steady states has been studied against step-type perturbation of different amplitudes. In Figs. 11 and 12 simulated dynamic response curves in the dimensionless time domain for dimensionless biomass concentrations (C^*_B) have been plotted using Eq. (31) against dimensionless residence time, $\tau^*(=1/D^*)$ considering the amplitude of perturbation as a parameter. The experimental results have been superimposed on the same set of curves in both the figures. It is evident that the experimental data match appreciably well with the simulated curves with sufficiently high index of correlation (index of correlation: 0.9756–0.9972 (Fig. 11); 0.9770–0.9988 (Fig. 12)). Thus, it may be concluded that the proposed model is good enough to predict the experimental results to a high degree of accuracy.

The transient behavior of a culture to approach a new steady state/around a steady state can give information about the response of the culture to perturbation in operating conditions. In Figs. 11 and 12, the transient response of culture due to step-type perturbations of different amplitudes (1%, 5%, 10%, 30%, and 70% of the original value) in $C_{A,in}$ are shown. As expected, new steady state values for biomass depend on degree of per-

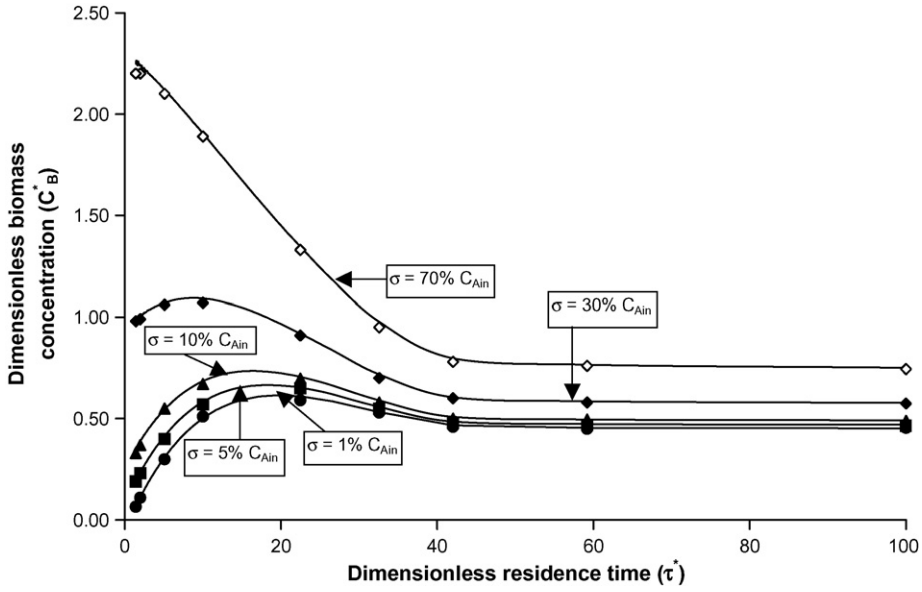

Fig. 11. Simulated (—) and experimental ((●) $\sigma = 1.0\%$ $C_{A,in}$; (■) $\sigma = 5.0\%$ $C_{A,in}$; (▲) $\sigma = 10.0\%$ $C_{A,in}$; (♦) $\sigma = 30.0\%$ $C_{A,in}$; (◊) $\sigma = 70.0\%$ $C_{A,in}$) dynamic responses for dimensionless biomass concentration (C^*_B) against dimensionless residence time (τ^*) with fractional step change in $C_{A,in}$ (σ) as a parameter. In all cases $C_{A,in} = 1.696$ g/dm^3.

turbation. Furthermore, the nature of response also depends on the degree of perturbation. It is clear from Fig. 11 that the characteristic time, i.e., the time required to achieve the new steady states is almost the same for each case of perturbation above 10% for higher inlet substrate concentration originally at 1.696 g/dm^3. Value of characteristic time is almost 40 residence time. On the other hand, from the close observation of Fig. 12 it is evident that when the steady state originally obtained for substrate concentration of 0.904 g/dm^3 is perturbed new steady states are reached after 25 residence time for all amplitudes of perturbation. It is evident from Figs. 11 and 12 that with the increase in the amplitude of step change in $C_{A,in}$, an overshoot is observed in the profile of dimensionless biomass concentration against dimensionless residence time upto 30% perturbation. Above this range the value of C^*_B decreases monotonically until a new steady state is attained. This may be due to the fact that when the amplitude of perturbation in $C_{A,in}$ is upto 30%, the biomass initially shows a tendency to increase due to its formation in larger proportion. Subsequently as the product is formed in appreciable quantity due to enhanced supply of substrate from feed stream, this biomass formation is inhibited by the product. On the other hand, when the value of $C_{A,in}$ is beyond a certain limit (above 30% perturbation) the enhanced production rate of biomass is suppressed by the product inhibition effect from the

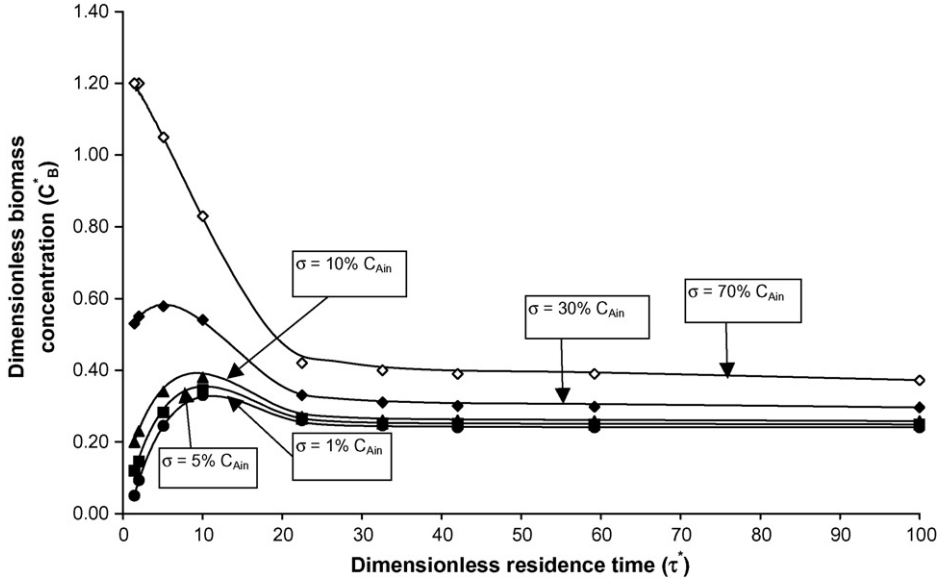

Fig. 12. Simulated (—) and experimental ((●) $\sigma = 1.0\%$ $C_{A,in}$; (■) $\sigma = 5.0\%$ $C_{A,in}$; (▲) $\sigma = 10.0\%$ $C_{A,in}$; (♦) $\sigma = 30.0\%$ $C_{A,in}$; (◊) $\sigma = 70.0\%$ $C_{A,in}$) dynamic responses for dimensionless biomass concentration (C^*_B) against dimensionless residence time (τ^*) with fractional step change in $C_{A,in}$ (σ) as a parameter. In all cases $C_{A,in} = 0.904$ g/dm^3.

very initial moment. As a consequence, the non-dimensional time–concentration profiles of biomass always follow a monotonically declining pattern until new steady states are reached. Extent of overshoot obtained in case of lower original substrate concentration (0.904 g/dm^3) is larger than that obtained in case of higher (1.696 g/dm^3) one. This may be due to the fact that at lower range of substrate concentration product generated in the system inhibits the microbial growth in lower extent in comparison to that at higher concentration.

5. Conclusion

This paper presents an experimental and modeling study of microbial reduction of SO_2, the first step of microbial reduction of SO_2 to elemental sulfur. The main focus of the present investigation is on non-ideality, steady state stability and dynamic response. Non-ideal behavior of the chemostat has been assessed using a two-parameter model, namely, bypass and dead volume concepts. Under the present set of values of operating parameters the bioreactor has been observed to behave ideally. Stability and dynamic studies can be robust tests for bioreactor models. Models those survive such tests could be applied with some confidence outside laboratory conditions specifically for designing of industrial bioreactors. Stability and dynamic studies have been undergone using traditional linear stability analysis and phase plane analysis. Appropriate forcing functions (inlet substrate concentration and dilution rate) have been used. The whole scheme has been based upon presently generated experimental data as well as previously published work [3–15].

References

[1] W.A. Apel, J.M. Barnes, M.R. Weibe, Removal of sulfur dioxide from combustion gas streams using sulfate reducing bacteria, Bioprocess Eng. Symp. (1992) 83–88.
[2] B.N. Dasu, V. Deshmane, R. Shanmugasundram, C.M. Lee, K.L. Sublette, Microbial reduction of sulfur dioxide and nitric oxide, Fuel 72 (1993) 1705–1714.
[3] A. Ajbar, I. Gamal, Stability and bifurcation of an unstructured model of a bioreactor with cell recycle, Math. Comput. Model. 25 (1997) 31–48.
[4] A. Ajbar, K. Alhumaizi, Microbial competition: study of global branching phenomena, AIChE J. 46 (2000) 321–334.
[5] A. Ajbar, K. Alhumaizi, Biodegradation of substitutable substrates in a continuous bioreactor with cell recycle: a study of static bifurcation, Math. Comput. Model. 31 (2000) 159–174.
[6] A. Ajbar, Classification of static behaviour of a class of unstructured models of continuous bioprocesses, Biotechnol. Prog. 17 (2001) 597–605.
[7] A. Ajbar, Classification of stability behavior of bioreactors with wall attachment and substrate-inhibited kinetics, Biotechnol. Bioeng. 72 (2001) 166–176.
[8] A. Ajbar, Stability analysis of the biodegradation of mixed wastes in a continuous bioreactor with cell recycle, Water Res. 35 (2001) 1201–1208.
[9] A. Ajbar, On the existence of oscillatory behavior in unstructured models of bioreactor, Chem. Eng. Sci. 56 (2001) 1991–1997.
[10] D. DiBiasio, in: M.L. Shuler (Ed.), Chemical Engineering Problems in Biotechnology, American Institute of Chemical Engineers, New York, 1989, pp. 265–299.
[11] H.W. Blanch, D.S. Clark, Biochemical Engineering, Marcel Dekker Inc., New York, 1997.
[12] A.J. Daugulis, P.J. McLellan, J. Li, Experimental investigation and modeling of oscillatory behavior in the continuous culture of *Zymomonas mobilis*, Biotechnol. Bioeng. 56 (1997) 99–105.
[13] J.H. Lee, J. Hong, H.C. Lim, Experimental optimization of fed-batch culture for poly-β-hydroxybutyric acid production, Biotechnol. Bioeng. 56 (1997) 697–705.
[14] V.M. Saucedo, M.N. Karim, Experimental optimization of a real time fed-batch fermenter process using Markov decision process, Biotechnol. Bioeng. 55 (1997) 317–327.
[15] Z.L. Xiu, A.P. Zeng, W.D. Deckwer, Multiplicity and stability analysis of microorganisms in continuous culture: effects of metabolic overflow and growth inhibition, Biotechnol. Bioeng. 57 (1998) 251–261.
[16] H.S. Fogler, Elements of Chemical Reaction Engineering, 2nd ed., Prentice-Hall of India Pvt. Ltd., 1992.
[17] J.R. Postgate, The Sulphate Reducing Bacteria, 2nd ed., Cambridge University Press, Cambridge, 1984.
[18] F.D. Snell, L.S. Ettre (Eds.), Encyclopedia of Industrial Chemical Analysis, John Wiley & Sons Inc., 1973, pp. 360–440.
[19] J.E. Bailey, D.F. Ollis, Biochemical Engineering Fundamentals, 2nd ed., McGraw Hill Inc., Singapore, 1986.
[20] M.L. Shuler, F. Kargi, Bioprocess Engineering—Basic Concepts, Pearson Education, Inc., New Jersey, 2000.
[21] A.D. Myškis, Advanced Mathematics for Engineers (Translated from Russian) (M. Volosov, I.G. Volosova, Trans.), Mir Publishers, Moscow, 1979.
[22] W.L. Luyben, Process Modeling Simulation and Control for Chemical Engineers, 2nd ed., McGraw Hill, Inc., New York, 1990.